

**Influence of terminal substitution on structural, DNA, Protein binding, anticancer and antibacterial activities of palladium(II) complexes containing 3-methoxy salicylaldehyde-4(N) substituted thiosemicarbazones†**P. Kalaivani,<sup>a</sup> R. Prabhakaran,<sup>\*a,b</sup> E. Ramachandran,<sup>a</sup> F. Dallemer,<sup>b</sup> G. Paramaguru,<sup>c</sup> R. Renganathan,<sup>c</sup> P. Poornima,<sup>d</sup> V. Vijaya Padma<sup>d</sup> and K. Natarajan<sup>\*a</sup>

Received 28th September 2011, Accepted 1st November 2011

DOI: 10.1039/c1dt11838b

The variable chelating behavior of 3-methoxysalicylaldehyde-4(N)-substituted thiosemicarbazones was observed in equimolar reactions with [PdCl<sub>2</sub>(PPh<sub>3</sub>)<sub>2</sub>]. The new complexes were characterized by various analytical, spectroscopic techniques (mass, <sup>1</sup>H-NMR, absorption, IR). All the new complexes were structurally characterized by single crystal X-ray diffraction. Crystallographic results showed that the ligands H<sub>2</sub>L<sup>1</sup> and H<sub>2</sub>L<sup>4</sup> are coordinated as binategative tridentate ONS donor ligands in the complexes **1** and **4** by forming six and five member rings. However, the ligands H<sub>2</sub>L<sup>2</sup> and H<sub>2</sub>L<sup>3</sup> bound to palladium in **2** and **3** as uninegative bidentate NS donors by forming a five member chelate ring. From this study, it was found that the substitution on terminal 4(N)-nitrogen may have an influence on the chelating ability of thiosemicarbazone. The presence of hydrogen bonding in **2** and **3** might be responsible for preventing the coordination of phenolic oxygen to the metal ion. The interaction of the complexes with calf-thymus DNA (CT-DNA) has been explored by absorption and emission titration methods. Based on the observations, an electrostatic binding mode of DNA has been proposed. The protein binding studies were monitored by quenching of tryptophan and tyrosine residues in the presence of complexes using Lysozyme as model protein. Antibacterial activity studies of the complexes have been screened against pathogenic bacteria such as *Enterococcus faecalis*, *Staphylococcus aureus*, *Escherichia coli*, *Klebsiella pneumonia* and *Pseudomonas aeruginosa*. MIC50 values of the complexes showed that they exhibited significant activity against the pathogens and among them, **3** exhibited higher activity. Further, anticancer activity of the complexes on the lung cancer cell line A549 has also been studied.

**1. Introduction**

Among the sulfur family, thiosemicarbazones are unique and multifaceted ligands that possess a variety of flexible donor sets and are capable of coordinating to the metal ion through the sulfur and one of the hydrazinic nitrogen atoms (N1 or N2), leading to the formation of either a five or a four member chelate ring.<sup>1,2</sup>

<sup>a</sup>Department of Chemistry, Bharathiar University, Coimbatore, 641 046, India. E-mail: rpnchemist@gmail.com, k\_natraj6@yahoo.com; Fax: +91-422-2422387; Tel: +91-422-2428319

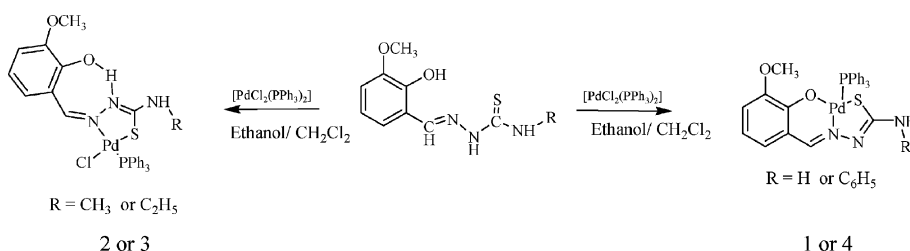
<sup>b</sup>Laboratoire Chimie Provence-CNRS UMR6264, Université of Aix-Marseille I, II and III – CNRS, Campus Scientifique de Saint-Jérôme, Avenue Escadrille Normandie-Niemen, F-13397, Marseille, Cedex 20, France

<sup>c</sup>Department of Chemistry, Bharathidasan University, Trichirappalli, 620 015, India

<sup>d</sup>Department of Biotechnology, Bharathiar University, Coimbatore, 641 046, India

† Electronic supplementary information (ESI) available. CCDC reference numbers 815366–815369 for [Pd(Msal-tsc)(PPh<sub>3</sub>)](**1**), [Pd(H-Msal-mtsc)Cl(PPh<sub>3</sub>)](**2**), [Pd(H-Msal-etse)Cl(PPh<sub>3</sub>)](**3**) and [Pd(Msal-ptsc)(PPh<sub>3</sub>)](**4**). For ESI and crystallographic data in CIF or other electronic format see DOI: 10.1039/c1dt11838b

The versatility of the thiosemicarbazone ligands for binding to the metal ion has been well documented. Besides the enormous structural diversity exhibited by the metal complexes,<sup>3</sup> they possess a wide range of biological properties such as antiviral,<sup>4</sup> antifungal,<sup>5</sup> antibacterial,<sup>6</sup> antitumor,<sup>7</sup> anticarcinogenic<sup>8</sup> and insulin mimetic properties.<sup>9</sup> For the last decade, our group has been actively engaged in the synthesis and characterization of N-substituted thiosemicarbazone complexes with various transition metals.<sup>2d,2h,10</sup> In the continuation of our efforts in understanding the coordination propensities of thiosemicarbazones, we have carried out the structural characterization of new palladium(II) complexes containing 3-methoxysalicylaldehyde-4(N)-substituted thiosemicarbazones (H<sub>2</sub>L<sup>1-4</sup>). The study on the interaction of transition metal complexes with DNA is a vibrant area of research.<sup>11</sup> In this area, the ability to selectively target and cleave DNA with high affinity and to report on the binding event by changes in luminescence is of great current interest.<sup>12</sup> An advantage of using transition metal complexes in such studies is that the ligands and metal ions in such complexes can be conveniently varied to suit individual applications due to the ability to inhibit the biosynthesis of DNA, possibly by binding to the nitrogen base of DNA or



**Scheme 1** Preparation of new palladium(II) complexes.

RNA, which may hinder or block base replication.<sup>13</sup> Cisplatin is one of the most widely used anticancer drugs.<sup>14</sup> In general, nuclear DNA is the cellular target associated with the therapeutic action of cisplatin.<sup>15</sup> One of the major drawbacks of the platinum anticancer drugs is its resistance, either developed or intrinsic.<sup>16</sup> Phenoxide compounds appended with thiosemicarbazone pharmacophore have been known to exert cytotoxicities towards many cancer cells. With the above facts in mind, new palladium(II) complexes containing substituted thiosemicarbazones have been synthesized, characterized and their cytotoxicity has been tested on lung cancer cell line A549 and also been subjected to test their potential activity against various pathogenic bacteria such as *Enterococcus faecalis*, *Staphylococcus aureus*, *Escherichia coli*, *Klebsiella pneumonia* and *Pseudomonas aeruginosa*. In this paper, we are reporting the synthesis, characterization, crystallography, DNA, protein binding ability and cytotoxic activities of new Pd(II) thiosemicarbazone complexes.

## 2. Results and discussion

The reaction between  $[\text{PdCl}_2(\text{PPh}_3)_2]$  and a series of 4(N)-substituted thiosemicarbazones ( $\text{H}_2\text{L}^{1-4}$ ) in 1:1 ethanol/dichloromethane resulted in the formation of new complexes (Scheme 1), the analytical data of which confirmed the stoichiometry of the complexes (**1–4**). The complexes are soluble in common organic solvents such as dichloromethane, chloroform, benzene, acetonitrile, ethanol, methanol, dimethylformamide and dimethylsulfoxide.

### Spectroscopic studies

The IR spectra of the ligands  $\text{H}_2\text{L}^{1-4}$  and the corresponding complexes provided significant information about the metal ligand bonding. A band in the region  $3339\text{--}3458\text{ cm}^{-1}$  due to a hydrogen bonded  $\text{--OH}$  group in the free ligands ( $\text{H}_2\text{L}^{1-4}$ ) was not observed in the IR spectra of complexes **1** and **4**. This indicates that the phenolic oxygen is deprotonated and coordinated in the complexes **1** and **4**. This was further supported by the increase in the value of phenolic  $\text{C--O}$  stretching frequency from  $1272$  to  $1307\text{ cm}^{-1}$  and  $1273$  to  $1313\text{ cm}^{-1}$  in the complexes **1** and **4**.<sup>10a</sup> However, the  $\nu_{(\text{O--H})}$  stretching frequency found at  $3424$  and  $3310\text{ cm}^{-1}$  for the complexes **2** and **3** indicated the non-participation of phenolic oxygen in coordination to the palladium ion. A strong vibration observed at  $1536\text{--}1593\text{ cm}^{-1}$  in the ligands corresponding to  $\nu_{(\text{C=N})}$  was shifted to  $1582\text{--}1596\text{ cm}^{-1}$  in all the complexes indicating the participation of azomethine nitrogen in bonding.<sup>17</sup> A sharp band observed at  $771\text{--}795\text{ cm}^{-1}$ , ascribed to  $\nu_{(\text{C=S})}$  in the

ligands  $\text{H}_2\text{L}^{1-4}$ , has completely disappeared in the spectra of all the new complexes and the appearance of a new band at  $739\text{--}743\text{ cm}^{-1}$  due to  $\nu_{(\text{C--S})}$  indicated the coordination of the sulfur atom after enolisation followed by deprotonation.<sup>2b</sup> Moreover, the characteristic absorption bands due to triphenylphosphine were also present in the expected region.<sup>18</sup> The electronic spectra of the complexes have been recorded in dichloromethane and they displayed three to five bands in the region around  $234\text{--}418\text{ nm}$ . The bands appearing in the region  $234\text{--}386\text{ nm}$  have been assigned to intra ligand transition<sup>19</sup> and the bands around  $394\text{--}418\text{ nm}$  have been assigned to ligand to metal charge transfer transitions.<sup>19a,20</sup> The  $^1\text{H-NMR}$  spectra of  $\text{H}_2\text{L}^{1-4}$  and the corresponding complexes recorded in DMSO showed all the expected signals (Fig. S1–S8†). In the spectra of  $\text{H}_2\text{L}^{1-4}$ , a singlet appearing in the range  $9.13\text{--}10.0\text{ ppm}$  has been assigned to the N(2)HCS group.<sup>21</sup> However, in the spectra of all the four complexes (**1–4**), there was no resonance attributable to N(2)H, indicating the coordination of ligands in the anionic form after deprotonation at N(2). A sharp singlet corresponding to the phenolic  $\text{--OH}$  group has appeared at  $11.34\text{--}11.76\text{ ppm}$  in the free ligands. In the spectra of **2** and **3** the appearance of a singlet at  $11.30\text{ ppm}$  indicated the non-participation of phenolic oxygen from coordination.<sup>2b</sup> But the same singlet has completely disappeared in **1** and **4**, confirming the involvement of phenolic oxygen in the coordination. In the spectra of  $\text{H}_2\text{L}^{1-4}$  and in all the four complexes, a complex multiplet appeared at  $6.48\text{--}7.7\text{ ppm}$  due to aromatic protons of the ligands and triphenylphosphine<sup>2b,2c</sup> and a singlet corresponding to the  $\text{--OCH}_3$  group occurred at the  $3.61\text{--}3.81\text{ ppm}$  range. Two singlets observed at  $8.37\text{--}8.40\text{ ppm}$  and  $8.37\text{--}9.40\text{ ppm}$  have been assigned to azomethine and terminal  $\text{--NH}$  protons for  $\text{H}_2\text{L}^{2-4}$ . Two broad singlets appeared at  $7.8$  and  $8.0\text{ ppm}$  corresponding to  $\text{NH}_2$  protons for  $\text{H}_2\text{L}^1$ . Though the spectra of **2** and **3** showed a singlet at  $8.3\text{--}8.5\text{ ppm}$  corresponding to the azomethine proton, the same has been observed as a doublet at  $8.2\text{--}8.6\text{ ppm}$  for **1** and **4**, which may be due to the coupling with the phosphorus atom of the triphenylphosphine.<sup>10b</sup> In the spectra of the complexes **2**, **3** and **4**, a sharp singlet was observed around  $7.74\text{--}8.40\text{ ppm}$  due to the terminal  $\text{--NH}$  protons of the substituted thiosemicarbazone ligands. In the spectra of  $\text{H}_2\text{L}^2$ ,  $\text{H}_2\text{L}^3$  and the complexes (**2** and **3**), a triplet was observed around  $1.03\text{--}2.90\text{ ppm}$  due to the methyl group of protons. In addition, a multiplet at  $3.12\text{--}3.58\text{ ppm}$  corresponding to the methylene group of protons was observed in the spectra of  $\text{H}_2\text{L}^3$  and **3**.<sup>22</sup> In order to confirm the composition of the new complexes, ES mass spectra were recorded in positive mode. The molecular ion peaks ( $\text{M}^+$ ) observed at  $m/z = 591, 668, 642$  and  $656$  supporting the molecular formulae. In addition, few representative fragment peaks were seen in the

spectra of all the four complexes. These fragments indicated the coordination of thiosemicarbazone ligands to the palladium metal atom.

### X-ray crystallography

Complex **1** crystallized in the triclinic space group  $P\bar{1}$  whereas the complexes **3** and **4** crystallized in the monoclinic space groups  $P2_1/c$  and  $P2_1$ , respectively. The complex **2** crystallized in the orthorhombic space group  $P2_12_12_1$ . The crystallographic data and bonding parameters and hydrogen bonding of the complexes are given in Tables 1–3. The molecular structures and hydrogen bonding diagrams are depicted in Fig. 1–7. In the complexes **1** and **4**, the Pd(II) ion is coordinated to the negatively charged tridentate ligand through the thiolate sulfur (Pd–S bond distances of 2.250(2) Å and 2.242(1) Å, respectively), phenolic oxygen (Pd–O bond distances of 2.010(6) Å and 2.020(4) Å, respectively) and the nitrogen atom (Pd–N bond distances of 2.014(8) Å and 2.019(4) Å, respectively). The remaining binding site is occupied by the triphenylphosphine unit (Pd–P(1) bond distances of 2.287(3) Å and 2.280(1) Å, respectively) with a bite angle [S(1)–Pd(1)–N(1)] of 83.6(2)° for **1** and 84.1(1)° for **4**. The [S(1)–Pd(1)–O(1)] bond angles found are 176.0(2)° for **1** and 176.5(1)° for **4** and the [P(1)–Pd(1)–N(1)] bond angles are 175.2(2)° for **1** and 172.2(1)° for **4**, which deviate considerably from the ideal angle of 180° causing significant distortion in the square planar geometry of the complexes. It is observed from the *trans* angle [P(1)–Pd(1)–N(1)] that the deviation from the ideal geometry is more in **4** than in **1**. In the complexes **2** and **3**, the mono basic bidentate ligand coordinated to Pd through the thiolate sulfur (Pd–S bond distances of 2.249(2) Å for **2** and 2.248(1) Å for **3**), and the nitrogen atom (Pd–N bond distances of 2.103(4) Å for **2** and 2.115(3) Å for **3**, respectively). The remaining binding sites are occupied by one chlorine atom (Pd–Cl bond distances of 2.338(2) Å for **2** and 2.341(1) Å for **3**, respectively) and the triphenylphosphine unit (Pd–P(1) bond distances of 2.259(2) Å for **2** and 2.269(1) Å for **3**) with the bite angle of 83.5(1) and 83.18(9), respectively, causing considerable distortion of the PdNSCIP coordination sphere. All the bond lengths fall in the range of reported values.<sup>2b</sup> The P(1)–Pd(1)–N(1) bond angles [171.6(1) for **2** and 176.11(9) for **3**] and Cl(1)–Pd(1)–S(1) bond angles [173.22(6) for **2** and 172.35(4) for **3**] deviate considerably from the ideal angle of 180°. The variation in *trans* angles in the complexes indicate considerable distortion from square planar geometry around palladium. In compound **1**, one of the hydrogen atoms of each amino group is engaged in intermolecular hydrogen bonding with the N2 nitrogen atom of a second molecule N(3A)–H(32A)···N(2B) and N(3B)–H(32B)···N(2A) (Fig. 2) and the second hydrogen is non bonded. This intermolecular hydrogen bonding gives a binuclear-like structural appearance. In complex **2**, two crystallographically distinct molecules are linked by hydrogen bonding. One is an intramolecular hydrogen bond, which is formed by an OH group (O(1A)···N(2A) 2.51(7) Å) while the second, which is intermolecular, is formed by the NH group (N(3A)···O(2) 2.98(7) Å. Symmetry code: (x, y, z); –1/2 + x, 1.5 – y, 1 – z; 1/2 + x, 1.5 – y, 1 – z; 1/2 + x, 1.5 – y, 1 – z; 1 + x, y, z. The complex **2** formed a layer structure through hydrogen bonding (Fig. 4). The result is the assembly of discrete complexes into a supramolecular 1D chain. In the complex **3**, one

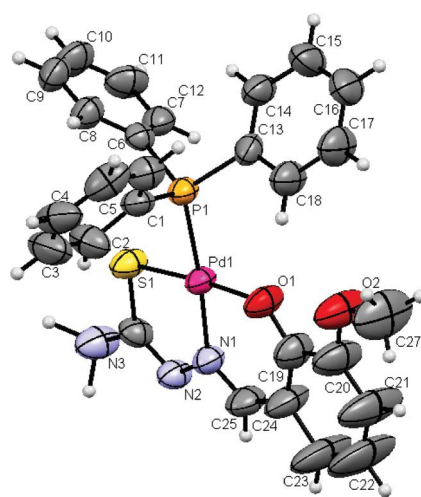


Fig. 1 ORTEP diagram of (1).

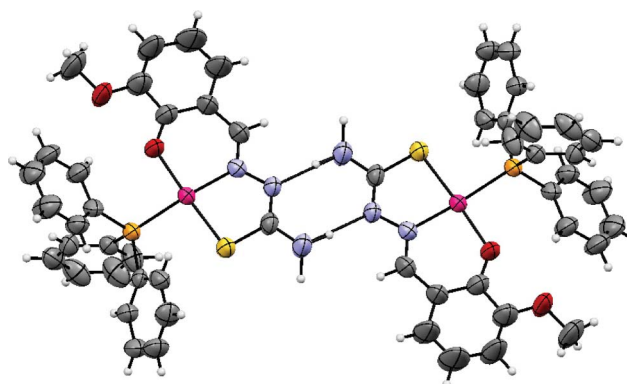


Fig. 2 ORTEP diagram of (1) with hydrogen bonding pseudo binuclear structure.

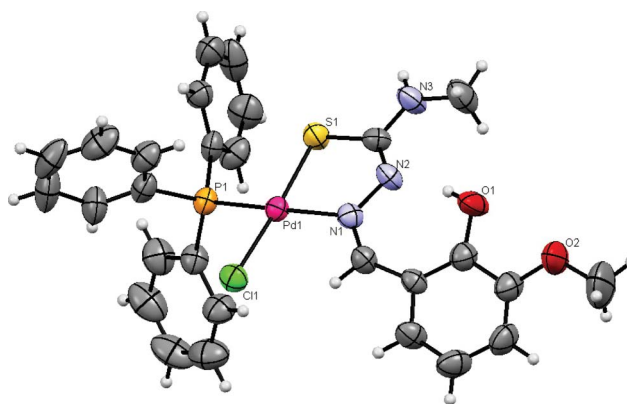


Fig. 3 ORTEP diagram of (2).

intra- and one intermolecular hydrogen bond were observed like in the case of **2**. This hydrogen bonding leads to the formation of 1D chain and each 1D chain is connected to two other chains through terminal NH groups and O donor atoms of adjacent complexes [N(3A)–H(3A)···O(2B) 3.03(0) Å], symmetry code: (x, y, z); 1 – x, –1/2 + y, 1.5 – z; 1 – x, 1/2 + y, 1.5 – z; x, –1 + y, z]. This net of hydrogen bonds allows the assembly of individual 1D chains into a zigzag 2D supramolecular network.

Table 1 Crystallographic data of new Pd(II) thiosemicarbazone complexes

	[Pd(Msal-tsc)(PPh <sub>3</sub> ) <sub>2</sub> ]	[Pd(H-Msal-mtsc)Cl(PPh <sub>3</sub> ) <sub>2</sub> ]	[Pd(H-Msal-etse)Cl(PPh <sub>3</sub> ) <sub>2</sub> ]	[Pd(MSal-ptsc)(PPh <sub>3</sub> ) <sub>2</sub> ]
Empirical formula	C <sub>27</sub> H <sub>24</sub> N <sub>3</sub> O <sub>2</sub> PPdS	C <sub>28</sub> H <sub>27</sub> ClN <sub>3</sub> O <sub>2</sub> PPdS	C <sub>29</sub> H <sub>29</sub> N <sub>3</sub> O <sub>2</sub> CIPdS	C <sub>33</sub> H <sub>28</sub> N <sub>3</sub> O <sub>2</sub> PPdS
Formula weight	591.04	642.41	656.43	668.01
Crystal system	Triclinic	Orthorhombic	Monoclinic	Monoclinic
Space group	<i>P</i> 1	<i>P</i> 2 <sub>1</sub> 2 <sub>1</sub>	<i>P</i> 2 <sub>1</sub> / <i>c</i>	<i>P</i> 2 <sub>1</sub>
Wavelength	0.71073 Å	0.71073 Å	0.71073 Å	0.71073 Å
Temperature	293 K	293 K	293 K	293 K
<i>a</i>	10.771(1) Å	9.8170(2) Å	14.9284(3) Å	11.9088(3) Å
<i>b</i>	11.8338(5) Å	14.5065(3) Å	10.2817(2) Å	8.0278(2) Å
<i>c</i>	12.1601(8) Å	21.6341(6) Å	18.9004(3) Å	15.6843(5) Å
<i>α</i>	69.422(2)°	90°	90°	90°
<i>β</i>	85.741(3)°	90°	102.443(1)°	102.480(1)°
<i>γ</i>	80.421(6)°	90°	90°	90°
<i>V</i>	1430.61(17) Å <sup>3</sup>	3080.92(12) Å <sup>3</sup>	2832.87(9) Å <sup>3</sup>	1464.01(7) Å <sup>3</sup>
Crystal size	0.10 × 0.12 × 0.16 mm	0.10 × 0.14 × 0.18 mm	0.12 × 0.20 × 0.25 mm	0.06 × 0.08 × 0.18 mm
<i>Z</i> value	2	4	4	2
Limiting indices	-13 ≤ <i>h</i> ≤ 11, -15 ≤ <i>k</i> ≤ 15, -15 ≤ <i>l</i> ≤ 13	-11 ≤ <i>h</i> ≤ 11, -17 ≤ <i>k</i> ≤ 18, -25 ≤ <i>l</i> ≤ 28	-16 ≤ <i>h</i> ≤ 20, -13 ≤ <i>k</i> ≤ 13, -24 ≤ <i>l</i> ≤ 23	-15 ≤ <i>h</i> ≤ 15, -08 ≤ <i>k</i> ≤ 10, -17 ≤ <i>l</i> ≤ 20
<i>D</i> <sub>calc</sub>	1.374	1.385	1.539	1.515
Reflections collected/unique	16172/3276 [ <i>R</i> <sub>int</sub> 0.078]	23445/4527 [ <i>R</i> <sub>int</sub> 0.0639]	23720/4239 [ <i>R</i> <sub>int</sub> 0.069]	13783/4927 [ <i>R</i> <sub>int</sub> 0.0665]
Theta range for data collection	1.86 to 28.17°	2.51 to 27.39°	1.4 to 28.72°	2.42 to 28.64°
<i>F</i> (000)	600	1304	1336	680
Goodness-of-fit on <i>F</i> <sup>2</sup>	0.958	1.011	0.931	0.847
Refinement method	Full-matrix least-squares on <i>F</i> <sup>2</sup>	Full-matrix least-squares on <i>F</i> <sup>2</sup>	Full-matrix least-squares on <i>F</i> <sup>2</sup>	Full-matrix least-squares on <i>F</i> <sup>2</sup>
<i>μ</i> (Mo-Kα)	0.804	0.836	0.911	0.795
Completeness to 2θ max	28.17°	27.39°	28.72°	28.64°
Data/restraints/parameters	6639/0/318	6623/0/337	7187/0/346	6913/1/371
Final <i>R</i> indices [ <i>I</i> > 2σ( <i>I</i> )]	<i>R</i> <sub>1</sub> = 0.078, <i>wR</i> <sub>2</sub> = 0.1773	<i>R</i> <sub>1</sub> = 0.099, <i>wR</i> <sub>2</sub> = 0.1124	<i>R</i> <sub>1</sub> = 0.1029, <i>wR</i> <sub>2</sub> = 0.1235	<i>R</i> <sub>1</sub> = 0.088, <i>wR</i> <sub>2</sub> = 0.0744
<i>R</i> indices (all data)	<i>R</i> <sub>1</sub> = 0.1692, <i>wR</i> <sub>2</sub> = 0.2071	<i>R</i> <sub>1</sub> = 0.0481, <i>wR</i> <sub>2</sub> = 0.0991	<i>R</i> <sub>1</sub> = 0.0421, <i>wR</i> <sub>2</sub> = 0.093	<i>R</i> <sub>1</sub> = 0.0477, <i>wR</i> <sub>2</sub> = 0.0658
Largest diff. peak and hole	0.668 and -0.894 e.Å <sup>-3</sup>	0.911 and -0.449 e.Å <sup>-3</sup>	0.741 and -0.93 e.Å <sup>-3</sup>	0.455 and -0.702 e.Å <sup>-3</sup>

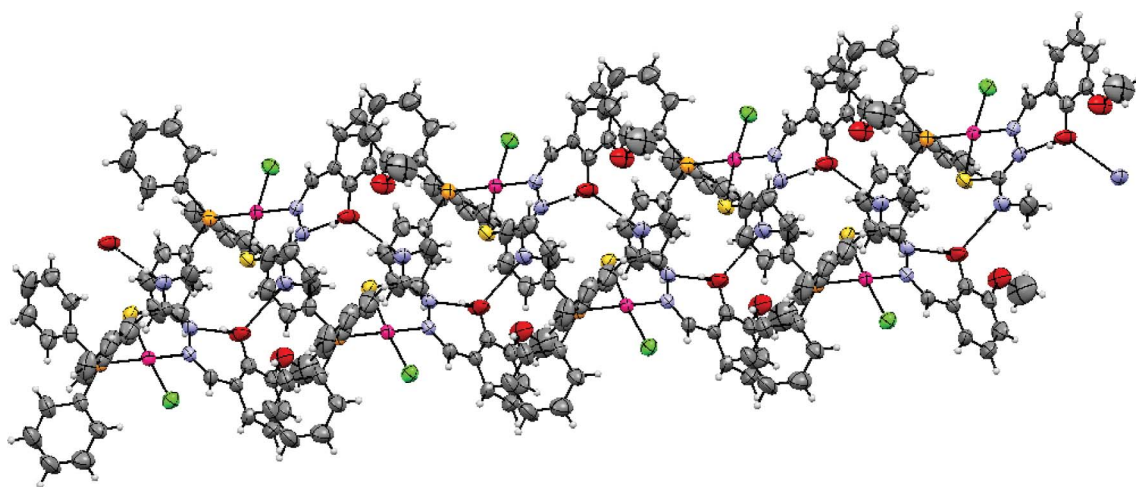
**Table 2** Selected bond lengths (Å) and angles (°) for Pd(II) thiosemicarbazone complexes

Atoms	[Pd(Msal-tsc)(PPh <sub>3</sub> )]	[Pd(H-Msal-mtsc)Cl(PPh <sub>3</sub> )]	[Pd(H-Msal-etsc)Cl(PPh <sub>3</sub> )]	[Pd(MSal-ptsc)(PPh <sub>3</sub> )]
Pd–S(1)	2.250(2)	2.250(2)	2.248(1)	2.242(1)
Pd–P(1)	2.287(3)	2.259(2)	2.269(1)	2.280(1)
Pd–O(1)	2.010(6)	—	—	2.020(3)
Pd–N(1)	2.014(8)	2.104(4)	2.115(3)	2.019(4)
Pd–Cl(1)	—	2.338(2)	2.341(1)	—
S(1)–Pd(1)–P(1)	92.63(8)	91.62(6)	93.16(4)	93.31(4)
S(1)–Pd(1)–O(1)	176.0(2)	—	—	176.5(1)
S(1)–Pd(1)–N(1)	83.6(2)	83.6(1)	83.18(9)	84.1(1)
P(1)–Pd(1)–O(1)	90.8(2)	—	—	90.1(1)
P(1)–Pd(1)–N(1)	175.2(2)	171.7(1)	176.11(9)	172.2(1)
O(1)–Pd(1)–N(1)	92.9(3)	—	—	92.5(1)
Cl(1)–Pd(1)–N(1)	—	95.6(1)	94.63(9)	—
Cl(1)–Pd(1)–P(1)	—	90.01(5)	88.83(4)	—
Cl(1)–Pd(1)–S(1)	—	173.25(6)	172.35(4)	—

**Table 3** Hydrogen bond lengths (Å) and angles (°) for 1–3

D–H...A	d(D–H)	d(H...A)	d(D...A)	<(DHA)
<b>1<sup>a</sup></b>				
N(3A)–H(32A)...N(2B)	1.14(4)	1.94(0)	3.08(1)	175.05
N(3B)–H(32B)...N(2A)	1.94(0)	1.14(4)	3.08(1)	175.05
<b>2<sup>b</sup></b>				
D–H...A	d(D–H)	d(H...A)	d(D...A)	<(DHA)
O(1A)–H(1A)...N(2A)	0.82(0)	1.70(9)	2.51(7)	167.91
N(3B)–H(3B)...O(1A)	0.86(0)	2.22(7)	2.98(7)	147.35
O(1B)–H(1B)...N(2B)	0.82(0)	1.70(9)	2.51(7)	167.91
N(3A)–H(3A)...O(1C)	0.86(0)	2.22(7)	2.98(7)	147.35
<b>3<sup>c</sup></b>				
D–H...A	d(D–H)	d(H...A)	d(D...A)	<(DHA)
O(1A)–H(1A)...N(2A)	0.82(0)	1.75(1)	2.55(3)	165.58
N(3A)–H(3A)...O(2B)	0.86(0)	2.17(3)	3.03(0)	174.01

<sup>a</sup> Symmetry operation for **1**: (x, y, z); (–x, –y, –z). <sup>b</sup> Symmetry operation for **2**: (x, y, z); –1/2 + x, 1.5 – y, 1 – z; 1/2 + x, 1.5 – y, 1 – z; 1/2 + x, 1.5 – y, 1 – z; 1 + x, y, z. <sup>c</sup> Symmetry operation for **3**: (x, y, z); 1 – x, –1/2 + y, 1.5 – z; 1 – x, 1/2 + y, 1.5 – z; x, –1 + y, z.

**Fig. 4** ORTEP diagram of (2) with hydrogen bonding 1D network.

### DNA binding studies

The interaction of transition metal complexes with DNA takes place *via* both covalent and/or non-covalent interactions.<sup>23</sup> In the case of covalent binding, the labile ligand of the complexes is replaced by a nitrogen base of DNA such as guanine N7, while the

non-covalent DNA interactions include intercalative, electrostatic and groove binding of metal complexes outside of the DNA helix. The DNA binding properties of the new Pd(II) complexes has been investigated by absorption and emission spectroscopy (Fig. 8a–8d). The spectra have been recorded for a constant CT-DNA concentration (3.5 μM) with different concentrations of complexes

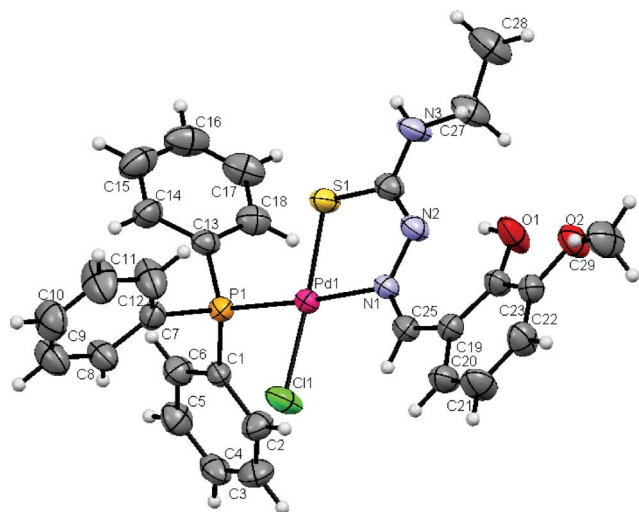


Fig. 5 ORTEP diagram of (3).

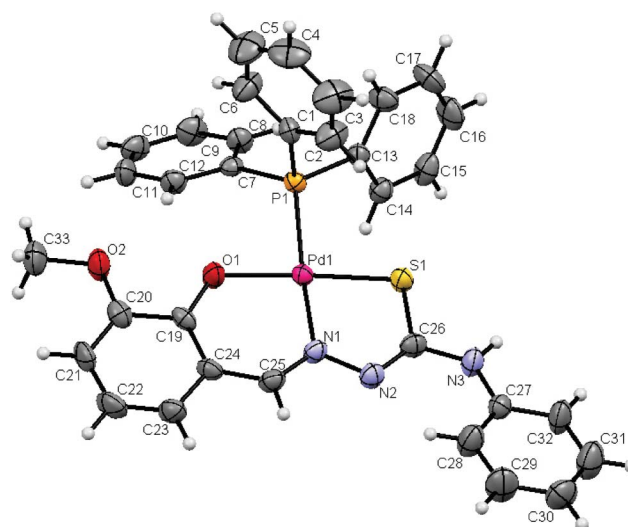


Fig. 7 ORTEP diagram of (4).

(1  $\mu\text{M}$ –40  $\mu\text{M}$ ). The changes observed in the absorption spectra of CT-DNA in the presence of various concentrations of these complexes, *i.e.* the increase of the intensity at  $\lambda_{\text{max}} = 262$  nm, which is accompanied with a blue shift of  $\lambda_{\text{max}}$  up to 232 nm, after mixing with each concentration of the new complexes (1–4), indicate that all the complexes had interaction with CT-DNA.

For complex 1, the intensity of the band at 262 nm ( $A = 0.1012$ ) for CT-DNA increased upon the addition of increasing concentrations of the complex (1  $\mu\text{M}$ –40  $\mu\text{M}$ ), while a blue shift was observed up to 242 nm ( $A = 1.5294$ ) accompanied by a hyperchromism (Fig. 8a). The binding behaviour of remaining complexes (2–4) is also quite similar. The band intensity of CT-DNA at  $\lambda_{\text{max}} = 262$  nm ( $A = 0.1012$ ) presents a blue shift up to 232 nm ( $A = 1.6126$ ) for 2, 232 nm ( $A = 1.8057$ ) for 3 and 240 nm ( $A = 1.9216$ ) for 4 (Fig. 8b–8d). The resultant hyperchromic shift suggests that all the complexes bind to CT-DNA by the external contact, possibly due to electrostatic binding.<sup>24</sup> The intrinsic binding constant  $K_b$  is a useful tool to monitor the magnitude of the binding strength of compounds with CT-DNA (Table 4). It can be determined by monitoring the changes in the absorbance at the corresponding  $\lambda_{\text{max}}$  with increasing concentration of the complex and is given by the ratio of slope to the Y intercept in plots of  $[\text{complex}]/(\epsilon_a - \epsilon_f)$  vs.  $[\text{complex}]$  (insets in Fig. 8a–8d). From the binding constant values, it is inferred that the complex 3 exhibited better binding than other complexes. Based on the  $K_b$  value, we can arrange the complexes in the following order with respect to

Table 4 Binding constant for interaction of complexes with CT-DNA

System	$K_b$ ( $\times 10^5 \text{ M}^{-1}$ )
CT-DNA + 1	0.502
CT-DNA + 2	1.445
CT-DNA + 3	1.697
CT-DNA + 4	0.230

the electron donating ability of the ligand *i.e.* the substitution on N-terminal nitrogen atom, 3 (ethyl) > 2 (methyl) > 1 (hydrogen) > 4 (phenyl).

In the emission spectra, the binding behaviour of complexes 1–4 is quite similar. The intensity of the band at  $\lambda_{\text{max}} = 289$  nm for CT-DNA is decreased from 1  $\mu\text{M}$  to 25  $\mu\text{M}$  by a blue shift for the complexes 1–4 (276, 257, 258 and 280 nm, respectively). The observed blue shift is an indication of hypsochromism resulting in electrostatic interaction between the complexes with CT-DNA. Further increase in the concentration of the complexes (30  $\mu\text{M}$ , 35  $\mu\text{M}$  and 40  $\mu\text{M}$ ) brought red shift with hypsochromism. This indicates, at higher concentrations of the complexes the binding mode turned from electrostatic to intercalative.

### Protein binding studies

**Fluorescence spectroscopy.** Qualitative analysis of the binding of complexes to lysozyme can be detected by examining the

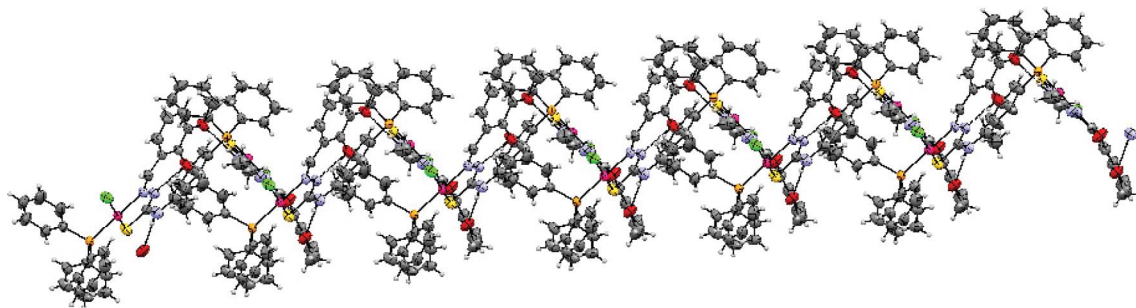
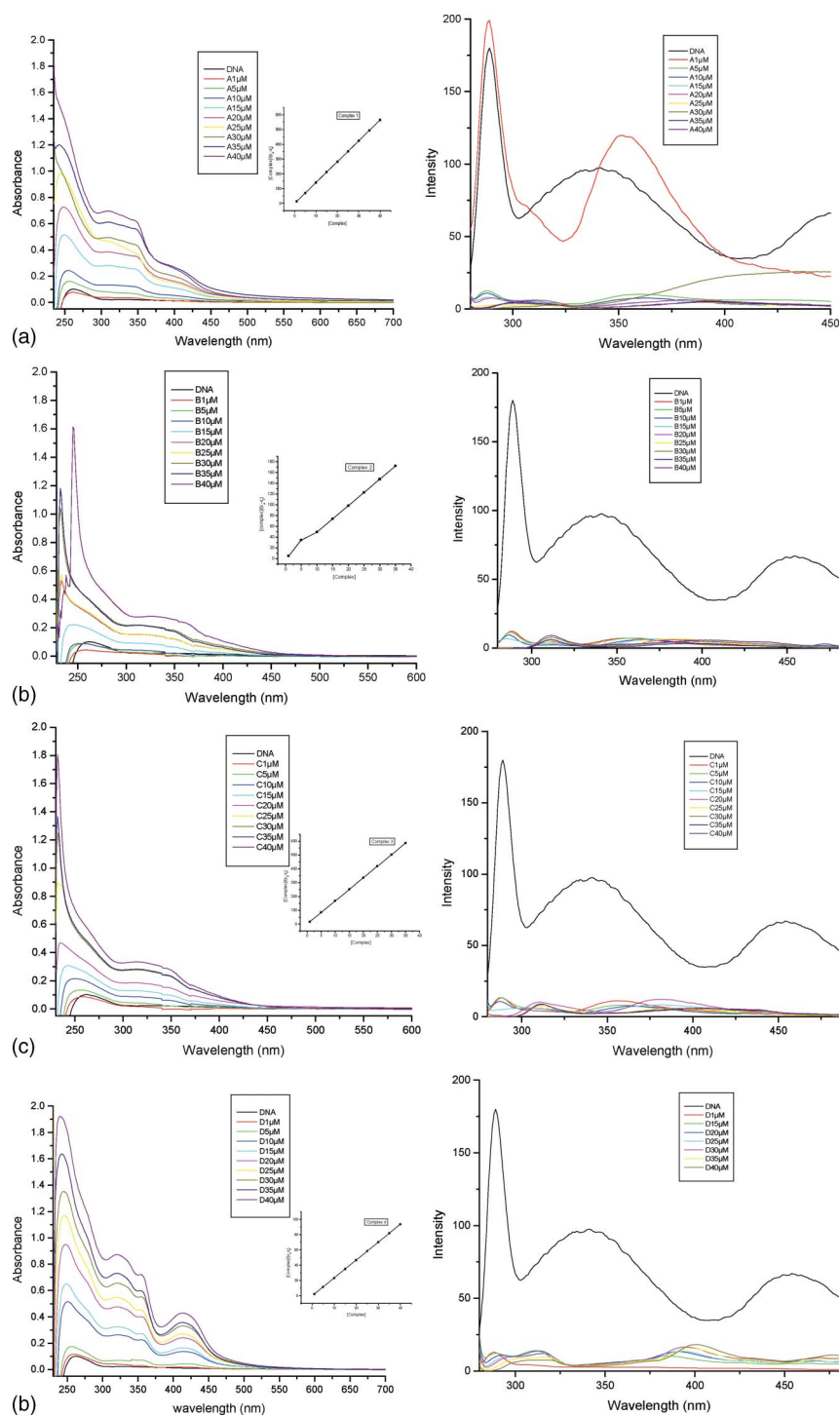


Fig. 6 ORTEP diagram of (3) with hydrogen bonding zigzag network.



**Fig. 8** (a) UV-vis and emission spectra of complex **1** in DMSO. (b) UV-vis and emission spectra of complex **2** in DMSO (c) UV-vis and emission spectra of complex **3** in DMSO. (d) UV-vis and emission spectra of complex **4** in DMSO.

emission spectra. Fluorescence measurements provide information about the binding of small molecules to a protein, such as the binding mechanism, binding mode, binding constants and binding sites. A variety of molecular interactions can result in quenching, including excited state reactions, molecular rearrangements, energy transfer, ground-state complex formation, and collisional quenching. The different mechanisms of quenching are

usually classified as either dynamic quenching or static quenching. Dynamic quenching refers to a process where the fluorophore and the quencher come into contact during the transient existence of the excited state. Static quenching refers to fluorophore–quencher complex formation.

The effect of the complex **4** on the photoluminescence intensity of lysozyme is shown in Fig. 9a. On increasing the concentration of

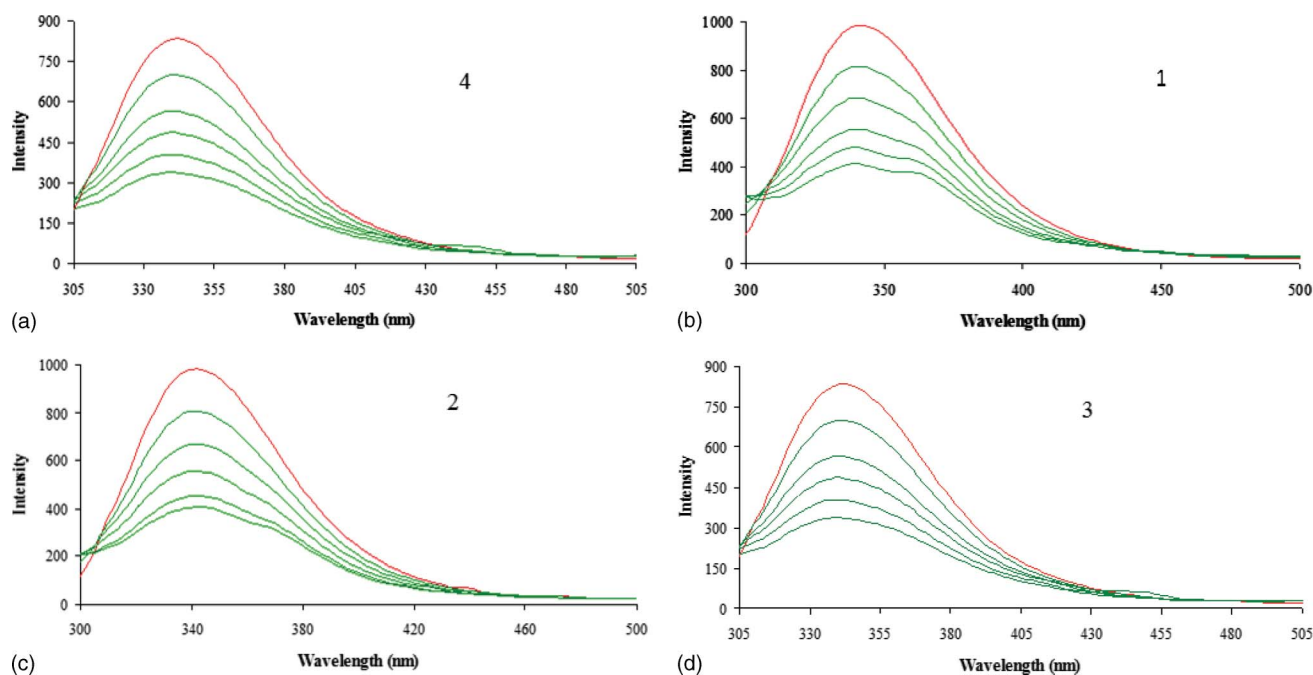


**Fig. 9** (a) The fluorescence quenching of lysozyme ( $1 \times 10^{-6}$  M;  $\lambda_{\text{exi}} = 280$  nm;  $\lambda_{\text{emi}} = 347$  nm) in the absence and presence of various concentrations of **4** ( $0-5 \times 10^{-5}$  M). (b) The fluorescence quenching of lysozyme ( $1 \times 10^{-6}$  M;  $\lambda_{\text{exi}} = 280$  nm;  $\lambda_{\text{emi}} = 347$  nm) in the absence and presence of various concentrations of **1** ( $0-5 \times 10^{-5}$  M). (c) The fluorescence quenching of lysozyme ( $1 \times 10^{-6}$  M;  $\lambda_{\text{exi}} = 280$  nm;  $\lambda_{\text{emi}} = 347$  nm) in the absence and presence of various concentrations of **2** ( $0-5 \times 10^{-5}$  M). (d) The fluorescence quenching of lysozyme ( $1 \times 10^{-6}$  M;  $\lambda_{\text{exi}} = 280$  nm;  $\lambda_{\text{emi}} = 347$  nm) in the absence and presence of various concentrations of **3** ( $0-5 \times 10^{-5}$  M).

complex **4**, a progressive decrease in the fluorescence intensity was observed, accompanied by a blue shift. The observed blue shift may be due to the binding of **4** with the active site in lysozyme.<sup>25</sup> This quenching effect indicates the interaction of lysozyme with **4**. The other complexes **1**, **2** and **3** also gave a similar type of fluorescence behavior (Fig. 9b–9d). The fluorescence quenching data have been analyzed by Stern Volmer equation (eqn (1)).

$$I_0/I = 1 + K_{\text{SV}} [Q] \quad (1)$$

Where  $I_0$  and  $I$  are the fluorescence intensities of the fluorophore in the absence and presence of quencher,  $K_{\text{SV}}$  is the Stern–Volmer quenching constant and  $[Q]$  is the quencher concentration. The plot of  $I_0/I$  vs.  $[Q]$  gave upward curvature suggesting the static nature of the quenching,<sup>26</sup> as shown in Fig. 10. Hence, the fluorescence quenching results from the formation of a complex between lysozyme and complex **4**.

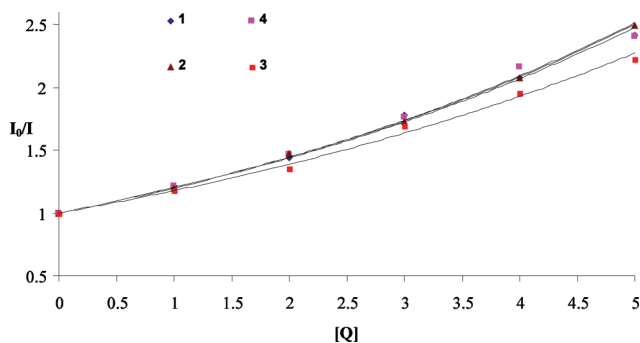


**Fig. 10** Plot of  $I_0/I$  vs.  $\log[Q]$ .

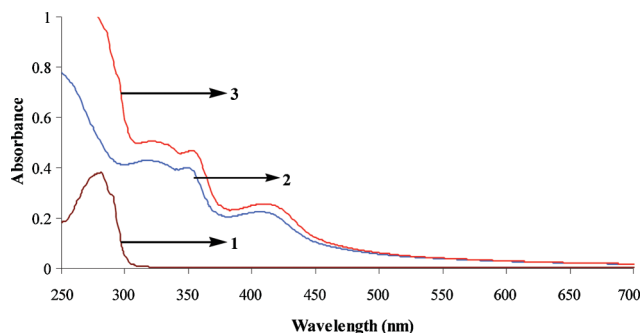
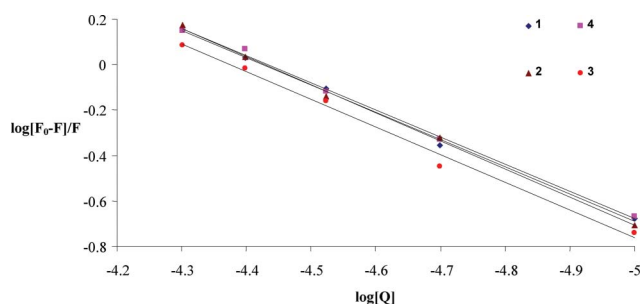
A common method to distinguish between static and dynamic quenching is by careful examination of the absorption spectra of the lysozyme in the presence of complexes. The absorption spectra of lysozyme, complex **4** and that of **4** + lysozyme have been depicted in Fig. 11. The changes in the absorbance spectra for **4** + lysozyme indicate that **4** interacts with the lysozyme. The absorption spectra of all the other complexes also show a similar type of change, which indicates their interaction with lysozyme. When small molecules bind to active site of Lysozyme, the equilibrium binding constant and the number of binding sites can be analyzed by using Scatchard equation (eqn (2)).

$$\log \left[ \frac{F_0 - F}{F} \right] = \log K + n \log [Q] \quad (2)$$

Where  $K$  is the binding constant of quencher with lysozyme,  $n$  is the number of binding sites,  $F_0$  and  $F$  are the fluorescence intensity in the absence and presence of the quencher. The value of  $K$  can be determined from the slope of the plot of  $\log[(F_0 - F)/F]$  vs.  $\log[Q]$  as shown in Fig. 12. The calculated value of the binding constant ( $K$ ) and the number of binding sites ( $n$ ) are listed in Table 5. The data obtained indicate that the complex **3** has higher magnitude of binding than **2**. This indicates that the binding ability to lysozyme increases by increasing the aliphatic chain in the amino group. Since all other groups are the same in both **3** and **2**, they differ only in the alkyl substituent. The free amino group in **1** has a lower binding value than the N-substituted complexes, which confirms the effect of substitution on binding with lysozyme. The complex **4**, which contains a phenyl substituent, has a similar binding constant to **1**. From this, it is inferred that the increase in electron donating ability of the substituent at the terminal nitrogen of the ligands

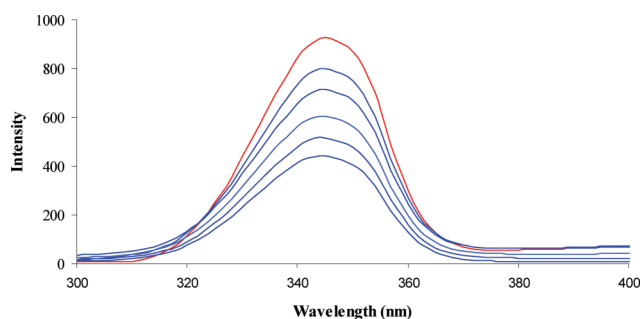
**Table 5** Binding constant and number of binding sites for interaction of complexes with lysozyme

System	$K (\times 10^5 \text{ M}^{-1})$	$n$
Lysozyme + <b>1</b>	1.98	1.1971
Lysozyme + <b>2</b>	2.06	1.2151
Lysozyme + <b>3</b>	3.07	1.2388
Lysozyme + <b>4</b>	1.94	1.1929

**Fig. 11** The absorption spectra of (1) Lysozyme ( $1 \times 10^{-6} \text{ M}$ ), (2) **4** ( $1 \times 10^{-5} \text{ M}$ ) and (3) Lysozyme + **4** [lysozyme =  $1 \times 10^{-6} \text{ M}$  and **4** =  $1 \times 10^{-5} \text{ M}$ ].**Fig. 12** Plot of  $\log[(F_0 - F)/F]$  vs.  $\log [Q]$ .

increases the protein binding ability of the complexes. This may be due to the increase in the electron density on the electron deficient metal centers.

The binding of small molecules to lysozyme could induce a conformational change of protein, because the intramolecular forces involved in maintaining the secondary structure could be altered. Spectroscopic methods are usually applied to study the conformation of protein. The fluorescence of lysozyme is due to tryptophan and tyrosine residues. Among them, tryptophan lies in the active site of the protein. Synchronous fluorescence spectra provide the information on the molecular microenvironment, particularly in the vicinity of the fluorophore functional groups.<sup>26</sup> In synchronous fluorescence spectroscopy, according to Miller,<sup>27</sup> the difference between excitation wavelength and emission wavelength ( $\Delta\lambda = \lambda_{\text{emi}} - \lambda_{\text{exc}}$ ) reflects the nature of the chromophores in the spectra. With larger  $\Delta\lambda$  values such as 60 nm, the synchronous fluorescence of lysozyme is characteristic of the tryptophan residue, while smaller  $\Delta\lambda$  values such as 15 nm are characteristic of tyrosine.<sup>28</sup> The synchronous fluorescence spectra of lysozyme with various concentrations of **4** were recorded at  $\Delta\lambda = 60 \text{ nm}$  and  $\Delta\lambda = 15 \text{ nm}$ . The fluorescence intensity of both tryptophan and tyrosine showed a decrease in intensity but the tryptophan spectrum is accompanied with blue shift (Fig. 13). It reveals that the binding around Trp residues is strengthened.

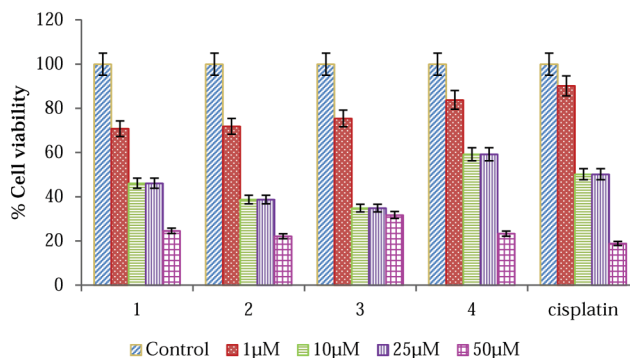
**Fig. 13** Synchronous spectra of lysozyme ( $1 \times 10^{-6} \text{ M}$ ) in the absence and presence of **4** ( $0-5 \times 10^{-5} \text{ M}$ ) in the wavelength difference of  $\Delta\lambda = 60 \text{ nm}$ .

Hence, the results clearly indicate that the complexes bind to the active site in the protein showing them as potential molecules for biological applications.

### Anticancer activity

Preliminary screening of anticancer activity for the new complexes was performed by MTT assay. All the samples were found to be cytotoxic to lung cancer cell line A549 (Fig. 14). The complex **3** showed higher cytotoxic effect followed by the complexes **1** and **2**. It is interesting to note that the complexes **1**, **2** and **3** exhibited better activity than cisplatin. The highest activity was noted for the complex **3** and the least activity was observed with the complex **4**. The  $\text{IC}_{50}$  value (50% inhibition of cell growth for 24 h) for the complexes **1-4** was determined as 18, 18, 15 and 30  $\mu\text{M}$ , respectively, and for cisplatin it was found as 25  $\mu\text{M}$ . The higher cytotoxic effects on lung cancer cells with lower  $\text{IC}_{50}$  values of the complexes indicate their efficiency in killing the cancer cells even at lower concentrations than the conventional standard cisplatin. Many researchers have reported the cytotoxicity effects of complexes with longer incubation period. But the present data shows that the complexes with lower incubation period with higher cytotoxic effects can replace the compounds that need longer time periods. As the longer incubation period may result in the development of cellular resistance for that particular compound and also have harmful effects such as affecting

### Cytotoxicity (MTT) Assay

**Fig. 14** The treatment of complexes exert an antiproliferative effect on lung cancer cells: A549 cells were treated with complexes (0.1, 1.0, 10, 25 and 50  $\mu\text{M}$ ) for 24 h. The control received appropriate carriers. Cell viability was assessed by MTT cell proliferation assay. The results shown are Mean  $\pm$  SD ( $n = 9$ ), which are three separate experiments performed in triplicate.

non-target sites in the body when they are used for clinical purposes, the compounds that show activity in shorter time periods are preferred. Our data are highly significant when compared with the results of Beckford *et al.*<sup>29</sup> They have reported the 50% inhibitory concentration of different complexes after exposure for 72 h in  $\mu\text{M}$  concentrations. Moreover, the  $\text{IC}_{50}$  values of our compounds are comparable with the reported  $\text{IC}_{50}$  values of standard anticancer drugs such as cisplatin and doxorubicin. As our samples are of high antiproliferative/anticancer activity, they may find their role in medicine. Further molecular studies are required to exploit our complexes in the pharmaceuticals.

### Cellular uptake study

The intracellular uptake of a specific drug plays a vital role in ameliorating treatment of several diseases. Since the  $\text{IC}_{50}$  values are critical when compared to the normal cells in the human body, the present study is focused on the concentrations that showed 50% inhibition for the lung cancer cells. The intracellular concentration of the complexes 1–4 and the standard doxorubicin were found out using the method described in the methodology.<sup>30</sup> The intracellular concentration of the complexes after the incubation period of 24 h was found to be 35.622, 49.938, 48.086 and 72.796%, respectively, for the complexes 1–4 and for the standard doxorubicin it was found as 59.16% (Fig. 15). With their  $\text{IC}_{50}$  values of 18, 18, 15, 30 and 5  $\mu\text{M}$ , the intracellular concentration of the different complexes used for the study was found to be approximately half of their  $\text{IC}_{50}$ . It is clear from the results that even a low concentration of the complexes is cytotoxic to the lung cancer cells when they are completely absorbed by the cells. Hence, further studies to improve their cellular uptake may be helpful for their use in the clinical world. A549 cells were treated with the different complexes for 24 h and their  $\text{IC}_{50}$  values and the concentrations of complexes in the cell lysates were measured with a fluorescence spectrophotometer at their maximum excitation/emission wavelengths. All the complexes entered the cancer cell, and the uptake levels were dependent on the dose of each complex used. This also indicated that their cytotoxicities as determined by the MTT assay were not disproportionately influenced by the complexes having different cellular uptake levels. Results in their percentage uptake are shown in Fig. 15, which are Mean  $\pm$  SD ( $n = 9$ ), in three separate experiments performed in triplicate.

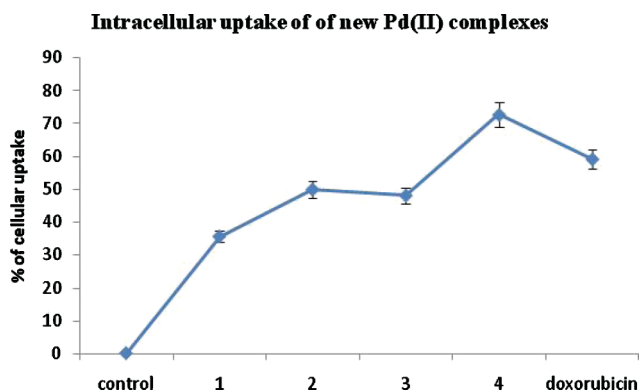


Fig. 15 Intracellular concentration of complexes in A549 cells.

### Antibacterial activity studies

Infections due to different pathogenic bacteria are a dreadful threat to the human race. Virulent strains of *E. coli* can cause gastroenteritis, urinary tract infections, and neonatal meningitis. *Enterococcus faecalis* can cause endocarditis, as well as bladder, prostate, and epididymal infections; nervous system infections are less common. In infants, the *S. aureus* infection can cause a severe disease staphylococcal scalded skin syndrome (SSSS), and it can cause mastitis in cows. *K. pneumoniae* leads to the dreadful disease pneumonia and *P. aeruginosa* is an opportunistic pathogen in immuno-compromised individuals.<sup>31–35</sup> Since these bacterial species develop resistance to the existing antibacterial agents, new compounds with more effective cytotoxic/cytostatic effects on the pathogenic bacteria are of urgent need in the medical field. There are hundreds of antibacterial agents but their use is limited due to a low spectrum of activity and good activity in high concentrations, which may also be toxic to the non targets. Antibacterial activities for palladium complexes have not been examined well. Here in our study, we made an attempt to explore the toxic effects of the newly synthesized palladium complexes on five different bacterial species. As described in the materials and methods, different concentrations of the complexes were used to find out their minimum inhibitory concentration on the bacterial species like *E. faecalis*, *S. aureus*, *E. coli*, *K. pneumoniae* and *P. aeruginosa*. Complex 3 was found to be more effective on *S. aureus*, *E. coli*, *K. pneumoniae* and *P. aeruginosa* with lower minimal inhibitory concentrations, followed by complex 2 (Fig. 16). Complex 1 was observed to be more toxic to *E. faecalis* when compared to the other three complexes. *E. faecalis* was sensitive to 2, 3 and 4 with the same inhibitory concentration. 4 and 1 showed similar minimum inhibitory concentrations on *E. coli* and *K. pneumoniae*. Complex 4 was observed to be less effective on *S. aureus* and *P. aeruginosa*. The activity for the metal chelates can be explained on the basis of chelation theory.<sup>36</sup> Chelation considerably reduces the polarity of the metal ion because of the partial sharing of its positive charge with the donor groups

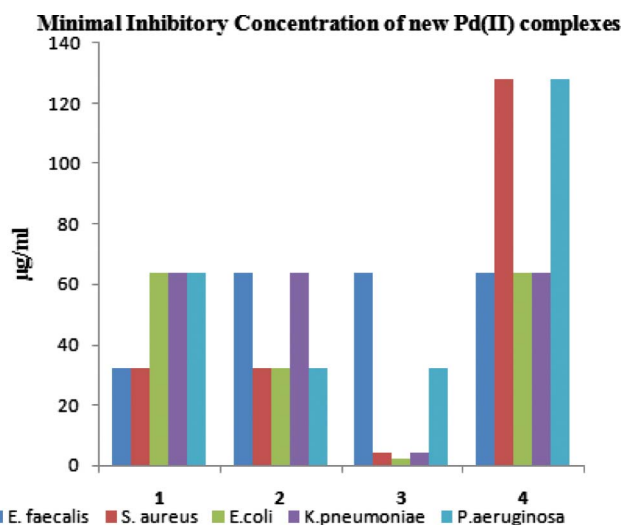


Fig. 16 Minimal inhibitory concentration of new Pd(II) complexes: the new Pd(II) complexes are exposed at different concentrations overnight and the minimal inhibitory concentration of each complex is given, considering that the control sets gave null values.

and possible  $\pi$ -electron delocalization over the chelate ring. Such chelation could increase the lipophilic character of the central metal atom, which subsequently favors the permeation through the lipid layer of cell membrane. The mode of action of the complexes may involve the formation of the hydrogen bond through the azomethine group ( $>C=N$ ) with the active centers of the cell constituents resulting in the interference with normal cell process.<sup>37</sup> The variation in the effectiveness of the different complexes against different organisms depends on the impermeability of the cells of microbes or difference in ribosome of the microbial cells.<sup>38</sup>

### 3. Conclusion

Various N-substituted thiosemicarbazones containing 3-methoxysalicylaldehyde were reacted with  $[PdCl_2(PPh_3)_2]$ . N-methyl and N-ethyl substituted thiosemicarbazones yielded palladium complexes with NS chelation by forming a stable five member ring with N(1) hydrazinic nitrogen and thiolate sulfur atoms. However, the unsubstituted and N-phenyl substituted thiosemicarbazones yielded the ONS chelate with the formation of five and six member rings by utilizing phenolic oxygen, N(1) nitrogen and thiolate sulfur atoms. The new complexes have been characterized by X-ray crystallography. Further, the complexes (**1–4**) have been subjected to DNA and protein binding studies. From the results, it is observed that the complexes significantly bind to the DNA and the protein. Among the complexes, **3** exhibited better binding affinity over the DNA and lysozyme. From the results of cytotoxicity studies, it is found that the complexes **1**, **2** and **3** exhibited better activity than the standard cisplatin. The complex **3** showed higher activity than the remaining complexes. In order to know the uptake of the complexes into the cells, cellular uptake studies were done and it was found that the uptake levels were dependent on the dose of each complex used. This designated that their cytotoxicities, as determined by the MTT assay, were not disproportionately influenced by the complexes having different cellular uptake levels. Antibacterial screening studies were also done to know about the effectiveness of the complexes on various pathogenic bacteria. All the complexes exhibited significant activity and the complex **3** showed better activity than all other complexes. From the overall results of the biological studies, the better activity of complex **3** may be due to the presence of more electron rich substitution on the terminal nitrogen. In general, the order of activity of the complexes may be assigned as **3** > **2** > **1** > **4**. Hence, it is concluded that the substitution on the N-terminal nitrogen may have a significant effect in tuning the structural and biological properties of the complexes formed in the given experimental condition.

### 4. Experimental

#### Materials

The ligands  $[H_2L^{1-4}]$  and the palladium complex  $[PdCl_2(PPh_3)_2]$  were synthesized according to the standard literature procedures.<sup>39</sup> All the reagents used were analar grade, were purified and dried according to the standard procedure.<sup>40</sup>

#### Synthesis of 3-methoxysalicylaldehyde thiosemicarbazone

##### $[H_2\text{-Msal-tsc}] (H_2L^1)$

Thiosemicarbazide (0.92 g, 10 mmol) was dissolved in 40 mL of methanol with continuous stirring and it was gently heated for a period of 30 min. To this, methanolic solution (10 mL) of 3-methoxy salicylaldehyde (1.53 g, 10 mmol) was added and the mixture was refluxed by stirring for 2 h. Upon cooling, a white crystalline product begins to separate. This was collected by filtration, washed well with cold methanol and dried in vacuum. The product dissolves in common organic solvents such as acetone, methanol, ethanol, dichloromethane, chloroform, DMF and DMSO. Yield: 38%. Anal. calcd for  $C_9H_{11}N_3O_2S$ : C 47.98; H 4.92; N 18.65; S 14.23. Found: C 47.76; H 5.00; N 18.67; S 14.20%. FT-IR ( $cm^{-1}$ ) in KBr: 3458 ( $\nu_{OH}$ ), 1593 ( $\nu_{C=N}$ ), 1272 ( $\nu_{C-O}$ ), 771 ( $\nu_{C=S}$ );  $^1H$  NMR (DMSO- $d_6$ , ppm): 11.36 (s, 1H, OH), 9.13 (s, 1H, NHCS), 8.38 (s, 1H, CH=N), 7.84 and 8.06 (2br s, 1H each,  $NH_2$ ), 3.79 (s, 3H,  $OCH_3$ ), 6.73–7.52 (m, 3H, aromatic).

A similar method as described above was followed for the preparation of all other thiosemicarbazone ligands.

##### 3-methoxysalicylaldehyde-4(N)-methylthiosemicarbazone

##### $[H_2\text{-Msal-mtsc}] (H_2L^2)$

The ligand  $[H_2\text{-Msal-mtsc}]$  was prepared from 4(N)-methylthiosemicarbazide (1.05 g, 10 mmol) and 3-methoxysalicylaldehyde (1.53 g, 10 mmol). Yield: 58%. Anal. Calcd for  $C_{10}H_{13}N_3O_2S$ : C, 50.19; H, 5.47; N, 17.56; S, 13.40. Found: C, 50.15; H, 5.40; N, 17.49; S, 13.31%. FT-IR ( $cm^{-1}$ ) in KBr: 3338 ( $\nu_{OH}$ ), 1554 ( $\nu_{C=N}$ ), 1276 ( $\nu_{C-O}$ ), 780 ( $\nu_{C=S}$ );  $^1H$  NMR (DMSO- $d_6$ , ppm): 11.40 (s, 1H, OH), 9.13 (s, 1H, NHCS), 8.37 (s, 1H,  $NHCH_3$ ), 8.36 (s, 1H, CH=N), 3.80 (s, 3H,  $OCH_3$ ), 6.75–7.54 (m, 3H, aromatic), 2.99 (d, 3H,  $CH_3$ ).

##### 3-methoxysalicylaldehyde-4(N)-ethylthiosemicarbazone

##### $[H_2\text{-Msal-etsc}] (H_2L^3)$

The ligand  $[H_2\text{-Msal-etsc}]$  was prepared from 4(N)-ethylthiosemicarbazide (1.19 g, 10 mmol) and 3-methoxysalicylaldehyde (1.53 g, 10 mmol). Yield: 64%. Anal. calcd for  $C_{11}H_{15}N_3O_2S$ : C 55.21; H 6.31; N 16.58; S 12.65. Found: C 55.15; H 6.27; N 16.50; S 12.59%. FT-IR ( $cm^{-1}$ ) in KBr: 3310 ( $\nu_{OH}$ ), 1536 ( $\nu_{C=N}$ ), 1276 ( $\nu_{C-O}$ ), 795 ( $\nu_{C=S}$ );  $^1H$  NMR (DMSO- $d_6$ , ppm): 11.34 (s, 1H, OH), 9.14 (s, 1H, NHCS), 8.42 (s, 1H,  $NHC_2H_5$ ), 8.40 (s, 1H, CH=N), 3.80 (s, 3H,  $OCH_3$ ), 6.75–7.53 (m, 3H, aromatic), 3.55–3.58 (m, 2H,  $CH_2$ ), 1.13 (t, 3H,  $CH_3$ ).

##### 3-methoxysalicylaldehyde-4(N)-phenylthiosemicarbazone

##### $[H_2\text{-Msal-ptsc}] (H_2L^4)$

The ligand  $[H_2\text{-Msal-ptsc}]$  was prepared from 4(N)-phenylthiosemicarbazide (1.67 g, 10 mmol) and 3-methoxysalicylaldehyde (1.53 g, 10 mmol). Yield: 54%. Anal. calcd for  $C_{15}H_{15}N_3O_2S$ : C 59.81; H 5.12; N 13.95; S 10.64. Found: C 59.65; H 4.99; N 13.78; S 10.43%. FT-IR ( $cm^{-1}$ ) in KBr: 3339 ( $\nu_{OH}$ ), 1589 ( $\nu_{C=N}$ ), 1273 ( $\nu_{C-O}$ ), 782 ( $\nu_{C=S}$ );  $^1H$  NMR (DMSO- $d_6$ , ppm): 11.76 (s, 1H, OH), 10.00 (s, 1H, NHCS), 9.20 (s, 1H,  $NHPh$ ), 8.50 (s, 1H, CH=N), 3.81 (s, 3H,  $OCH_3$ ), 6.76–7.68 (m, 8H, aromatic).

### Preparation of [Pd(Msal-tsc)(PPh<sub>3</sub>)] (1)

An ethanolic (25 mL) solution of [PdCl<sub>2</sub>(PPh<sub>3</sub>)<sub>2</sub>] (0.200 g; 0.285 mmol) was slowly added to 3-methoxysalicylaldehydethiosemicarbazone [H<sub>2</sub>-Msal-tsc] (0.064 g, 0.285 mmol) in dichloromethane (25 mL). The mixture was allowed to stand for 4 d at room temperature. A yellowish orange solid formed was filtered, washed with petroleum ether (60–80 °C) and recrystallized from dichloromethane and acetonitrile to yield orange red crystals. Yield: 55%. M.p. 236 °C. Anal. calcd. for C<sub>27</sub>H<sub>24</sub>N<sub>3</sub>O<sub>2</sub>SPdP: C 54.78; H 4.09; N 7.09; S 5.41. Found: C 54.70; H 4.01; N 7.00; S 5.38%. FT-IR (cm<sup>-1</sup>) in KBr: 1596 (ν<sub>C=N</sub>), 1307 (ν<sub>C-O</sub>), 742 (ν<sub>C-S</sub>), 1432, 1097, 695 cm<sup>-1</sup> (for PPh<sub>3</sub>); UV-vis (CH<sub>2</sub>Cl<sub>2</sub>), λ<sub>max</sub>: 234 (14879), 302 (9609), 342 (9900) nm (dm<sup>3</sup> mol<sup>-1</sup> cm<sup>-1</sup>) (intra-ligand transition); 394 (4931), 418 (2102) nm (dm<sup>3</sup> mol<sup>-1</sup> cm<sup>-1</sup>) (LMCT s→d); <sup>1</sup>H NMR (DMSO-d<sub>6</sub>, ppm): 8.24 (d (*J* = 14), 1H, CH=N), 3.60 (s, 3H, OCH<sub>3</sub>), 6.48–7.70 (m, aromatic), *m/z* = 592 (M<sup>+</sup>).

The very similar method was followed to synthesize other complexes.

### Preparation of [Pd(H-Msal-mtsc)(PPh<sub>3</sub>)] (2)

The complex **2** was prepared by the procedure as used for **1**, with 3-methoxy salicylaldehyde 4(N)-methylthiosemicarbazone [H<sub>2</sub>-Msal-mtsc] (0.068 g; 0.285 mmol) and [PdCl<sub>2</sub>(PPh<sub>3</sub>)<sub>2</sub>] (0.200 g; 0.285 mmol). Yield: 60%. M.p. 128 °C. Anal. calcd. for C<sub>28</sub>H<sub>27</sub>N<sub>3</sub>O<sub>2</sub>SCIPdP: C 52.38; H 4.23; N 6.54; S 4.99. Found: C 52.29; H 4.20; N 6.49; S 4.91%. FT-IR (cm<sup>-1</sup>) in KBr: 3424 (ν<sub>OH</sub>), 1593 (ν<sub>C=N</sub>), 1310 (ν<sub>C-O</sub>), 739 (ν<sub>C-S</sub>), 1437, 1097, 695 cm<sup>-1</sup> (for PPh<sub>3</sub>); UV-vis (CH<sub>2</sub>Cl<sub>2</sub>), λ<sub>max</sub>: 234 (24713), 316 (10965), 342 (8735), nm (dm<sup>3</sup> mol<sup>-1</sup> cm<sup>-1</sup>) (intra-ligand transition); 400 (4701) nm (dm<sup>3</sup> mol<sup>-1</sup> cm<sup>-1</sup>) (LMCT s→d); <sup>1</sup>H NMR (DMSO-d<sub>6</sub>, ppm): 11.30 (s, 1H, OH), 8.35 (s, 1H, CH=N), 8.39 (s, 1H, NHCH<sub>3</sub>), 3.61 (s, 3H, OCH<sub>3</sub>), 6.48–7.70 (m, aromatic), 2.72 (d (*J* = 4.8), 3H, CH<sub>3</sub>), *m/z* = 642 (M<sup>+</sup>).

### Preparation of [Pd(H-Msal-etsc)(PPh<sub>3</sub>)] (3)

The complex **3** was prepared by the procedure as used for **1**, with 3-methoxy salicylaldehyde 4(N)-ethylthiosemicarbazone [H<sub>2</sub>-Msal-etsc] (0.072 g; 0.285 mmol) and [PdCl<sub>2</sub>(PPh<sub>3</sub>)<sub>2</sub>] (0.200 g; 0.285 mmol). Yield: 65%. M.p. 234 °C. Anal. calcd for C<sub>29</sub>H<sub>29</sub>N<sub>3</sub>O<sub>2</sub>SCIPdP: C 53.06; H 4.45; N 6.40; S 4.88. Found: C 53.00; H 4.40; N 6.36; S 4.81%. FT-IR (cm<sup>-1</sup>) in KBr: 3317 (ν<sub>OH</sub>), 1582 (ν<sub>C=N</sub>), 1280 (ν<sub>C-O</sub>), 742 (ν<sub>C-S</sub>), 1450, 1092, 697 cm<sup>-1</sup> (for PPh<sub>3</sub>); UV-vis (CH<sub>2</sub>Cl<sub>2</sub>), λ<sub>max</sub>: 302 (14619), 338 (14113) nm (dm<sup>3</sup> mol<sup>-1</sup> cm<sup>-1</sup>) (intra-ligand transition); <sup>1</sup>H NMR (DMSO-d<sub>6</sub>, ppm): 11.30 (s, 1H, OH), 8.56 (s, 1H, CH=N), 7.74 (br s, 1H, NHC<sub>2</sub>H<sub>5</sub>), 3.77 (s, 3H, OCH<sub>3</sub>), 6.78–7.76 (m, aromatic), 3.12–3.15 (m, 2H, CH<sub>2</sub>), 1.03 (t, 3H, CH<sub>3</sub>), *m/z* = 656 (M<sup>+</sup>).

### Preparation of [Pd(Msal-ptsc)(PPh<sub>3</sub>)] (4)

The complex **4** was prepared by the procedure as used for **1**, with 3-methoxy salicylaldehyde 4(N)-phenylthiosemicarbazone [H<sub>2</sub>-Msal-ptsc] (0.086 g; 0.285 mmol) and [PdCl<sub>2</sub>(PPh<sub>3</sub>)<sub>2</sub>] (0.200 g; 0.285 mmol). Yield: 70%. M.p. 245 °C. Anal. calcd. for C<sub>33</sub>H<sub>28</sub>N<sub>3</sub>O<sub>2</sub>SPdP: C 59.33; H 4.22; N 6.29; S 4.80. Found: C 59.29; H 4.19; N 6.22; S 4.76%. FT-IR (cm<sup>-1</sup>) in KBr: 1594 (ν<sub>C=N</sub>), 1313

(ν<sub>C-O</sub>), 743 (ν<sub>C-S</sub>), 1433, 1098, 694 cm<sup>-1</sup> (for PPh<sub>3</sub>); UV-vis (CH<sub>2</sub>Cl<sub>2</sub>), λ<sub>max</sub>: 242 (54368), 292 (25117), 324 (29457), 348 (23960), nm (dm<sup>3</sup> mol<sup>-1</sup> cm<sup>-1</sup>) (intra-ligand transition); 412 (15475) nm (dm<sup>3</sup> mol<sup>-1</sup> cm<sup>-1</sup>) (LMCT s→d); <sup>1</sup>H NMR (DMSO-d<sub>6</sub>, ppm): 8.65 (d (*J* = 13.6), 1H, CH=N), 9.40 (s, 1H, NHPh), 3.64 (s, 3H, OCH<sub>3</sub>), 6.54–7.73 (m, aromatic), *m/z* = 668 (M<sup>+</sup>).

### Measurements

Infrared spectra were measured as KBr pellets on a Nicolet instrument between 400–4000 cm<sup>-1</sup>. Elemental analysis of carbon, hydrogen, nitrogen, and sulfur were determined using Vario EL III CHNS at the Department of Chemistry, Bharathiar University, Coimbatore, India. The electronic spectra of the complexes have been recorded in dichloromethane using a JASCO V-630 Spectrophotometer in the 200–800 nm range. Emission spectra were recorded by using a JASCO FP 6600 spectrofluorometer. <sup>1</sup>H NMR spectra were recorded in DMSO at room temperature with a Bruker 400 MHz instrument, chemical shift relative to tetramethylsilane. Melting points were measured in a Lab India apparatus.

### X-Ray crystallography

Single crystal data collections and corrections for the new Pd(II) complexes were done at 293 K with CCD kappa Diffractometer using graphite mono chromated Mo-Kα (λ = 0.71073 Å) radiation.<sup>41</sup> The structural solutions were done by using SHELXTL-97<sup>42</sup> and refined by full matrix least square on *F*<sup>2</sup> using SHELXL-97.<sup>43</sup>

### DNA binding studies

For electronic absorption titration, a stock of 1 mM solution of the complex was made up in a phosphate buffer (pH 7); 3000 μL of the solution was loaded into an optical glass cuvette with a path length of 1 cm, and 300 μL was removed with a micropipette and replaced with 300 μL of the complex solution. This cuvette was then loaded into the spectrometer sample block, controlled at 25 °C; 3000 μL of the buffer was loaded to an identical cuvette and placed in the reference cell. After the cuvettes had been allowed to reach equilibrium over the course of 30 min, a spectrum was recorded between 700 and 200 nm. Absorption titration experiments were performed by maintaining the nucleic acid (30 μL) concentration as constant (3.5 μM) and varying the metal complex concentration (1 μM–40 μM). The spectrum was recorded after checking for bubbles, which showed an increase in absorption indicating the interaction between the DNA and the metal complex. The intrinsic binding constant of the complex with CT-DNA was determined by using modified Stern volmer eqn (3).<sup>44,45</sup>

$$[\text{Complex}]/[\varepsilon_a - \varepsilon_f] = [\text{Complex}]/[\varepsilon_b - \varepsilon_f] + 1/K_b[\varepsilon_b - \varepsilon_f] \quad (3)$$

The absorption coefficients  $\varepsilon_a$ ,  $\varepsilon_f$ , and  $\varepsilon_b$  correspond to  $A_{\text{obsd}}/[\text{complex}]$ , the extinction coefficient for the free DNA and the extinction coefficient for the complex in the fully bound form, respectively. The slope and the intercept of the linear fit of the plot of  $[\text{Complex}]/[\varepsilon_a - \varepsilon_f]$  vs.  $[\text{Complex}]$  give  $1/[\varepsilon_a - \varepsilon_f]$  and  $1/K_b[\varepsilon_b - \varepsilon_f]$ , respectively. The intrinsic binding constant  $K_b$  can be obtained from the ratio of the slope to the intercept (Table 4).<sup>44</sup> Emission measurements were carried out by using a JASCO FP- 6600 spectrofluorometer. Tris-buffer was used as a blank to make preliminary adjustments. The excitation wavelength was

fixed and the emission range was adjusted before measurements. All measurements were made at 20 °C. For emission spectral titrations, DNA concentration was maintained constant as 3.5  $\mu\text{M}$  and the concentration of the palladium complex was varied from 1  $\mu\text{M}$  to 40  $\mu\text{M}$ . The emission enhancement factors were measured by comparing the intensities at the emission spectral maxima under similar conditions.

### Proteinase binding studies

Lysozyme was purchased from Hi Media, India. Lysozyme was prepared in phosphate buffer of pH 7.6 and stored in the dark at 4 °C for use. The concentration of lysozyme was determined spectrophotometrically using  $\epsilon_{280}$  (lysozyme) = 37 646  $\text{M}^{-1} \text{cm}^{-1}$ .<sup>46</sup> UV-vis absorption experiments were performed on JASCO V-630 spectrophotometer. Emission spectra were recorded on JASCO FP-6600 spectrofluorometer. The excitation wavelength of lysozyme was 280 nm and the emission was monitored at 342 nm. The excitation and emission slit widths (each 5 nm) and scan rate (500  $\text{nm min}^{-1}$ ) were maintained constant for all the experiments. A 3 mL solution, containing an appropriate concentration of lysozyme ( $1 \times 10^{-6}$  M) was titrated with successive additions of the complex. For synchronous fluorescence spectra, also the same concentration of Lysozyme and THPP were used and the spectra were measured at two different  $\Delta\lambda$  (difference between the excitation and emission wavelengths of lysozyme) values such as 15 and 60 nm.

### Cytotoxicity studies

The cytotoxic effect of the new palladium(II) complexes (1–4) along with the conventional standard cisplatin on lung cancer cells (A549) was assayed by the 3-(4,5-dimethylthiazol-2-yl)-2,5-diphenyltetrazolium bromide (MTT) assay.<sup>47</sup> The cells were seeded at a density of 10,000 cells per well, in 200  $\mu\text{L}$  of RPMI 1640 medium and were allowed to attach overnight in a  $\text{CO}_2$  incubator. Samples dissolved in DMSO were added to the cells at a final concentration of 1, 10, 25 and 50  $\mu\text{M}$  in the cell culture media. After 24 h, the wells were treated with 20  $\mu\text{L}$  of MTT (5  $\text{mg mL}^{-1}$  PBS) and incubated at 37 °C for 4 h. The purple formazan crystals formed were dissolved in 200  $\mu\text{L}$  of DMSO and read at 570 nm in a micro plate reader.

### Cellular uptake study

Cellular uptake of the complexes (1–4) was quantified along with the standard doxorubicin with a slight modification in the literature method.<sup>30</sup> Briefly, the lung cancer cells (A549) were treated with the different complexes for 24 h. The medium was aspirated and cells were washed thrice with ice cold PBS. Then, the cells were lysed with PBS containing 1% Triton X-100. The concentration of complexes in the cell lysates was measured with a fluorescence spectrophotometer (JASCO) at their maximum excitation/emission wavelengths of 300/440, 322/428, 302/427 and 350/461 nm, respectively, for 1, 2, 3 and 4. To offset the background fluorescence from the cellular components, separate standardization curves were prepared using cellular lysates containing a series of known concentrations of different complexes and the intracellular concentrations were found out using the standard curve.

### Antibacterial activity studies

MICs (minimum inhibitory concentration) of the compounds against test organisms such as *Enterococcus faecalis*, *Staphylococcus aureus*, *Escherichia coli*, *Klebsiella pneumonia* and *Pseudomonas aeruginosa* were determined by using the broth micro dilution method.<sup>48</sup> A broth microdilution susceptibility assay was used as recommended by NCCLS for the determination of the MIC. All the tests were performed in Mueller–Hinton broth (MHB) supplemented with Tween-80 detergent (final concentration of 0.5% (v/v)). Bacterial strains were cultured overnight at 37 °C in MHA. Test strains were suspended in MHB to give a final density of  $5 \times 10^5$   $\text{cfu mL}^{-1}$  and these were confirmed by viable counts. Geometric dilutions of the compounds were prepared in a 96-well microtiter plate, including one growth control (MHB + Tween 80) and one sterility control (MHB + Tween 80 + compound). The plates were incubated under normal atmospheric conditions at 37 °C for 24 h.

### Acknowledgements

Authors P.K. and K.N. gratefully acknowledge UGC-SAP and CSIR, India for the financial assistance and author R.P. gratefully acknowledge CNRS, France, for CNRS Fellowship.

### References

- (a) M. J. M. Campbell, *Coord. Chem. Rev.*, 1975, **15**, 279; (b) J. S. Casas, M. S. Garcia-Tasenda and J. Sordo, *Coord. Chem. Rev.*, 2000, **209**, 197.
- (a) F. Basuli, S. M. Peng and S. Bhattacharya, *Inorg. Chem.*, 1997, **36**, 5645; (b) F. Basuli, M. Ruf, C. G. Pierpont and S. Bhattacharya, *Inorg. Chem.*, 1998, **37**, 6113; (c) I. Pal, F. Basuli, T. C. W. Mak and S. Bhattacharya, *Angew. Chem., Int. Ed.*, 2001, **40**, 2923; (d) R. Prabhakaran, R. Karvembu, T. Hashimoto, K. Shimizu and K. Natarajan, *Inorg. Chim. Acta*, 2005, **358**, 2093; (e) L. M. Fostiak, I. Gracia, J. K. Swearingen, E. Bermejo, A. Castineivas and D. X. West, *Polyhedron*, 2003, **22**, 83; (f) L. Ze-Hua, D. Chun-Ying, L. Ji-Hui, L. Young-Jiang, M. Yu-Hua and Y. Xiao-Zeng, *New J. Chem.*, 2000, **24**, 1057; (g) S. B. Novakovi, G. A. Bogdanovic and V. M. Leovac, *Inorg. Chem. Commun.*, 2005, **8**, 9; (h) R. Prabhakaran, S. V. Renukadevi, R. Karvembu, R. Huang, J. Mautz, G. Huttner, R. Subashkumar and K. Natarajan, *Eur. J. Med. Chem.*, 2008, **43**, 268; (i) R. Prabhakaran, R. Sivasamy, J. Angayarkanni, R. Huang, P. Kalavani, R. Karvembu, F. Dallemer and K. Natarajan, *Inorg. Chim. Acta*, 2011, **374**, 674; (j) R. Prabhakaran, P. Kalavani, R. Huang, M. Sieger, W. Kaim, P. Viswanathamurthi, F. Dallemer and K. Natarajan, *Inorg. Chim. Acta*, 2011, **376**, 317.
- (a) F. Basuli, S. M. Peng and S. Bhattacharya, *Inorg. Chem.*, 2000, **39**, 1120; (b) D. Mishra, S. Naskar, M. G. B. Drew and S. K. Chattopadhyay, *Polyhedron*, 2005, **24**, 1861; (c) D. Mishra, S. Naskar, M. G. B. Drew and S. K. Chattopadhyay, *Inorg. Chim. Acta*, 2006, **359**, 585; (d) T. S. Lobana, A. P. S. Pannu, G. Hundal, R. J. Butcher and A. Castineiras, *Polyhedron*, 2007, **26**, 2621; (e) T. S. Lobana, S. Khanna, R. J. Butcher, A. D. Hunter and M. Zeller, *Inorg. Chem.*, 2007, **46**, 5826; (f) T. S. Lobana, G. Bawa, A. Castineiras, R. J. Butcher and M. Zeller, *Organometallics*, 2008, **27**, 175; (g) T. S. Lobana, R. Sharma, G. Bawa and S. Khanna, *Coord. Chem. Rev.*, 2009, **253**, 977; (h) R. Pedrido, A. M. González-Noya, M. J. Romero, M. Martínez-Calvo, M. V. López, E. Gómez-Fórneas, G. Zaragoza and M. R. Bermejo, *Dalton Trans.*, 2008, 6776; (i) B. Ülküseven, T. Bal-Demirci, M. Akkurt, S. P. Yalçın and Ö. Büyükgüngör, *Polyhedron*, 2008, **27**, 3646; (j) Y. Kang, N. Yang, S. O. Kang and J. Ko, *Organometallics*, 1997, **16**, 5522; (k) I. G. Santos, U. Abram, R. Alberto, E. V. Lopez and A. Sanchez, *Inorg. Chem.*, 2004, **43**, 1834.
- (a) C. Q. Debra, A. K. Kathy and R. K. Earl, *Antiviral Res.*, 2006, **71**, 24; (b) Y. Teitz, D. Ronen, A. Vansover, T. Stematsky and J. L. Riggs, *Antiviral Res.*, 1994, **24**, 305.

- 5 M. C. Rodriguez-Arguelles, E. C. Lopez-Silva, J. Sanmartin, P. Pelagatti and F. Zani, *J. Inorg. Biochem.*, 2005, **99**, 2213.
- 6 (a) M. C. Rodriguez-Arguelles, E. C. Lopez-Silva, J. Sanmartin, A. Bacchi, C. Pelizzi and F. Zani, *Inorg. Chim. Acta*, 2004, **357**, 2543; (b) A. Cukurovali, I. Yilmaz, S. Gur and C. Kazaz, *Eur. J. Med. Chem.*, 2006, **41**, 201.
- 7 (a) A. Murugkar, B. Unnikrishnan, S. Padhye, R. Bhonde, S. Teat, E. Triantafyllou and E. Sinn, *Met.-Based Drugs*, 1999, **6**, 177; (b) Y. Teitz, N. Barko, M. Abramoff and D. Ronen, *Chemotherapy*, 1994, **40**, 195.
- 8 (a) W. X. Hu, W. Zhou, C. Xia and X. Wen, *Bioorg. Med. Chem. Lett.*, 2006, **16**, 2213; (b) Z. Afrasiabi, E. Sinn, S. Padhye, S. Dutta, S. Padhye, C. Newton, C. E. Anson and A. K. Powell, *J. Inorg. Biochem.*, 2003, **95**, 306; (c) T. Bal, B. Atasever, Z. Solakoglu, S. Erdem-Kuruca and B. Ulkuseven, *Eur. J. Med. Chem.*, 2007, **42**, 161.
- 9 M. Campana, C. Laborie, G. Barbier, R. Assan and R. Milcent, *Eur. J. Med. Chem.*, 1991, **26**, 273.
- 10 (a) R. Prabhakaran, V. Krishnan, K. Pasumpon, D. Sukanya, E. Wendel, C. Jayabalakrishnan, H. Bertagnolli and K. Natarajan, *Appl. Organomet. Chem.*, 2006, **20**, 203; (b) R. Prabhakaran, R. Huang, R. Karvembu, C. Jayabalakrishnan and K. Natarajan, *Inorg. Chim. Acta*, 2007, **360**, 691; (c) R. Prabhakaran, R. Huang, S. V. Renukadevi, R. Karvembu, M. Zeller and K. Natarajan, *Inorg. Chim. Acta*, 2008, **8**, 2547; (d) M. Muthukumar, S. Sivakumar, P. Viswanathamurthi, R. Karvembu, R. Prabhakaran and K. Natarajan, *J. Coord. Chem.*, 2010, **63**, 296; (e) S. Gowri, M. Muthukumar, S. Krishnaraj, P. Viswanathamurthi, R. Prabhakaran and K. Natarajan, *J. Coord. Chem.*, 2010, **63**, 524; (f) K. P. Balasubramanian, R. Karvembu, R. Prabhakaran, V. C. Chinnusamy and K. Natarajan, *Spectrochim. Acta.*, 2007, **68A**, 50; (g) V. C. Chinnusamy and K. Natarajan, *Synth. React. Inorg. Met.-Org. Chem.*, 1993, **23**, 889; (h) R. Prabhakaran, P. Kalaivani, R. Jayakumar, M. Zeller, A. D. Hunter, S. V. Renukadevi, E. Ramachandran and K. Natarajan, *Metallomics*, 2011, **3**, 42; (i) P. Kalaivani, R. Prabhakaran, F. Dallemer, P. Poornima, E. Vaishnavi, E. Ramachandran, V. Vijaya Padma, R. Renganathan and K. Natarajan, *Metallomics*, 2012, DOI: 10.1039/C1MT00144B.
- 11 (a) B. M. Zeglis, V. C. Pierre and J. K. Barton, *Chem. Commun.*, 2007, 4565; (b) D. S. Sigman, A. Mazumder and D. M. Perrin, *Chem. Rev.*, 1993, **93**, 2295.
- 12 (a) J. G. Vos and J. M. Kelly, *Dalton Trans.*, 2006, 4869; (b) K. E. Erkkila, D. T. Odom and J. K. Barton, *Chem. Rev.*, 1999, **99**, 2777; (c) C. Moucheron, A. Kirsch-De Mesmaeker and J. M. Kelly, *J. Photochem. Photobiol., B*, 1997, **40**, 91; (d) M. J. Hannon, *Chem. Soc. Rev.*, 2007, **36**, 280; (e) C. Metcalfe and J. A. Thomas, *Chem. Soc. Rev.*, 2003, **32**, 215.
- 13 R. A. Finch, M. C. Liu, S. P. Grill, W. C. Rose, R. Loomisa, K. M. Vasquez, Y. C. Cheng and A. C. Sarforelli, *Biochem. Pharmacol.*, 2000, **59**, 983.
- 14 (a) E. Wong, *Chem. Rev.*, 1999, **99**, 2451; (b) T. W. Hambley, *Coord. Chem. Rev.*, 1997, **166**, 181; (c) J. Reedijk, *Chem. Commun.*, 1996, 801; (d) B. A. J. Jansen, J. V. D. Zwan, H. D. Dulk and J. Reedijk, *J. Med. Chem.*, 2001, **44**, 245.
- 15 E. R. Jamleson and S. J. Lippard, *Chem. Rev.*, 1999, **99**, 2467.
- 16 (a) L. R. Kelland, *Crit. Rev. Oncol. Hematol.*, 1983, **15**, 191; (b) D. P. Gately and S. B. Howell, *Br. J. Cancer*, 1993, **67**, 1171.
- 17 D. X. West, I. S. Billeh, J. P. Jasinski, J. M. Jasinski and R. J. Butcher, *Transition Met. Chem.*, 1998, **23**, 209.
- 18 R. Karvembu, S. Hemalatha, R. Prabhakaran and K. Natarajan, *Inorg. Chem. Commun.*, 2003, **6**, 486.
- 19 (a) Y. P. Tiam, C. Y. Duan, Z. L. Lu and X. Z. You, *Polyhedron*, 1996, **15**, 2263; (b) S. Dey, V. K. Jain, A. Kwoedler and W. Kaim, *Ind. J. Chem.*, 2003, **42A**, 2339.
- 20 D. M. Boghaei and S. Mohebi, *J. Chem. Res.*, 2001, 224.
- 21 T. S. Lobana, A. Sanchez, J. S. Casas, A. Castineiras, J. Sordo, M. S. Garciaasende and E. M. Vazquez-Lopez, *J. Chem. Soc., Dalton Trans.*, 1997, 4289.
- 22 D. L. Klayman, J. P. Scovill and J. F. J. Brtosevich, *J. Med. Chem.*, 1983, **26**, 35.
- 23 Q. L. Zhang, J. G. Liu, H. Chao, G. Q. Xue and L. N. Ji, *J. Inorg. Biochem.*, 2001, **83**, 49.
- 24 (a) E. C. Long and J. K. Barton, *Acc. Chem. Res.*, 1990, **23**, 271; (b) R. F. Pasternack, E. J. Gibbs and J. J. Villafranca, *Biochemistry*, 1983, **22**, 251.
- 25 Y. J. Hu, Y. O. Yang, C. M. Dai, Y. Liu and X. H. Xiao, *Biomacromolecules*, 2010, **11**, 106.
- 26 G. Z. Chen, X. Z. Huang, J. G. Xu, Z. B. Wang and Z. Z. Zhang, *Method of Fluorescent Analysis*, second ed., Science Press, Beijing, 1990, p. 123 (Chapter 4).
- 27 J. N. Miller, *Proc. Anal. Div. Chem. Soc.*, 1979, **16**, 203.
- 28 E. A. Brustein, N. S. Vedenkina and M. N. Irkova, *Photochem. Photobiol.*, 1973, **18**, 263.
- 29 F. A. Beckford, M. Shaloski, G. Leblanc, J. Thessing, L. C. Lewis-Alleyne, A. A. Holder, L. Li, L. Navindra and P. Seeram, *Dalton Trans.*, 2009, 10757.
- 30 X. B. Xiong, Z. Ma, R. Lai and A. Lavasanifar, *Biomaterials*, 2010, **31**, 757.
- 31 K. Todar, *Pathogenic E. coli. Online Textbook of Bacteriology*, University of Wisconsin–Madison Department of Bacteriology.
- 32 L. L. Pelletier, *Microbiology of the Circulatory System in: Baron's Medical Microbiology*, S. Baron et al., ed., 4th ed., Univ. of Texas Medical Branch, 1996, ISBN 0-9631172-1-1.
- 33 K. J. Ryan and C. G. Ray, *Sherris Medical Microbiology*, 4th ed., McGraw Hill, 2004, 294. ISBN 0-8385-8529-9.
- 34 J. P. Curran and F. L. Al-Salihi, *Pediatrics*, 1980, **66**, 285 PMID 6447271.
- 35 B. T. Cenci-Goga, M. Karama, P. V. Rossitto, R. A. Morgante and J. S. Cullor, *J. Food Protection*, 2003, **66**, 1693 PMID 14503727.
- 36 B. G. Tweedy, *Phytopathology*, 1964, **55**, 910.
- 37 R. Prabhakaran, A. Geetha, M. Thilagavathi, R. Karvembu, V. Krishnan, H. Bertagnolli and K. Natarajan, *J. Inorg. Biochem.*, 2004, **98**, 2131.
- 38 P. G. Lawrence, P. L. Harold and O. G. Francis, *Antibiotics and Chemotherapy*, 1957, **4**, 1980.
- 39 (a) S. Purohit, A. P. Koley, L. S. Prasad, P. T. Manoharan and S. Ghosh, *Inorg. Chem.*, 1989, **28**, 3735; (b) J. L. Burmeister and F. Basolo, *Inorg. Chem.*, 1964, **3**, 1587.
- 40 A. I. Vogel, *Textbook of Practical Organic Chemistry*, 5<sup>th</sup> ed., Longman, London, 1989, 268.
- 41 (a) R. H. Blessing, *Acta Crystallogr., Sect. A: Found. Crystallogr.*, 1995, **51**, 33; (b) R. H. Blessing, *Crystallogr. Rev.*, 1987, **1**, 3; (c) R. H. Blessing, *J. Appl. Crystallogr.*, 1989, **22**, 396.
- 42 G. M. Sheldrick, *SHELXTL Version 5.1, An Integrated System for Solving, Refining and Displaying Crystal Structures from Diffraction Data*, Siemens Analytical X-ray Instruments, Madison, WI, 1990.
- 43 G. M. Sheldrick, *SHELXL-97, Program for refinement of crystal structures*, University of Göttingen, Germany, 1997.
- 44 A. Wolfe, G. H. Shimer and T. Meehan, *Biochemistry*, 1987, **26**, 6392.
- 45 G. Cohen and H. Eisenberg, *Biopolymers*, 1969, **8**, 45.
- 46 C. N. Pace, F. Vajdos, L. Fee, G. Grimsley and T. Gray, *Protein Sci.*, 1995, **4**, 2411.
- 47 T. Mossman, *J. Immunol. Methods*, 1983, **65**, 55.
- 48 NCCLS, National Committee for Clinical Laboratory Standards, Performance Standards for Antimicrobial Disk Susceptibility Test, 6th ed., Approved Standard, Wayne, PA, M2-A6, 1997.